IEEE Access
Multidisciplinary | Rapid Review | Open Access Journal

Received August 18, 2019, accepted August 28, 2019, date of publication September 9, 2019,
date of current version September 25, 2019.

Digital Object Identifier 10.1109/ACCESS.2019.2938831

An Improvement of the Performance of SAR Offset Tracking Approach to Measure Optimal Surface Displacements

SUNG-HO CHAE[1], WON-JIN LEE[1,2], WON-KYUNG BAEK[1], AND HYUNG-SUP JUNG[1], (Senior Member, IEEE)

[1]Department of Geoinformatics, University of Seoul, Seoul 02504, South Korea
[2]Environmental Satellite Center, National Institute of Environmental Research, Incheon 22689, South Korea

Corresponding author: Hyung-Sup Jung (hsjung@uos.ac.kr)

This work was supported in part by the Korea Meteorological Administration Research and Development Program under Grant KMI2017-9060, and in part by the Research Fund of National Institute of Environmental Research (NIER) under Grant NIER2019-01-01-028.

ABSTRACT For the measurement of abrupt and large surface movements caused by earthquakes, volcanic eruption and melting glacier, Synthetic aperture radar (SAR) offset tracking method would be a feasible solution because it can provide unambiguous ground displacements in both the ground range and azimuth directions when the interferometric phase is not coherent. However, the measurement performance of the method largely depends on the kernel size, which denotes the size of search window to estimate the azimuth and range offsets between reference and target SAR images. Thus, there is a trade-off between sensitivity and measurement density depending on the search kernel size. In this study, an enhanced SAR offset tracking method based on multi-kernel processing has been developed to find an optimized measurement from the trade-off between resolution and measurement accuracy. It can obtain optimal surface displacement measurements by calculating multiple offset measurements and determining a final measurement from the statistical properties of the multiple measurements. The measurement performance of the proposed method was evaluated by using European Remote Sensing 2 (ERS-2) satellite SAR data sets of the Hector Mine earthquake event in 1999 and Advanced Land Observing Satellite-2 Phased Array type L-band Synthetic Aperture Radar-2 (ALOS-2 PALSAR-2) data sets of the 2016 Kumamoto earthquake event. Our results showed that an optimized measurement from the trade-off between the observation accuracy and resolution can be effectively determined by our proposed processing strategy. The results are improved results for measurement density and accuracy over previously published results. It further confirmed that our new method is allowed for the optimal measuring the large-scale fast surface displacements that cannot be sufficiently observed with the phase-based SAR method.

INDEX TERMS Synthetic aperture radar (SAR), SAR offset tracking, surface deformation measurements, the 1999 hector mine earthquake, the 2016 Kumamoto earthquake.

I. INTRODUCTION

Surface deformation mapping is very important because it is a fundamental information to acquire detailed knowledge about the mechanism of geological activities. Synthetic aperture radar (SAR) interferometry (InSAR) technique has been shown to be a feasible technique for mapping that allows for the precise measurement of surface deformation (millimeter-to meter-level deformation) over a large area running at thousands of square kilometers [1]–[3]. However, because the InSAR method can only measure deformation along the antenna's line-of sight (LOS) direction, it has a limitation of one-dimensional (1D) deformation mapping. Moreover, when the surface displacements are very fast, the deformation rate exceeds the maximum detectable deformation rate of one fringe. Thus, the InSAR method has difficulties to measure fast ground deformation because of lack of coherence.

The associate editor coordinating the review of this manuscript and approving it for publication was Junjie Wu.

On the contrary, SAR offset tracking method, especially intensity tracking, can overcome the weakness of the phase-based InSAR method. It can measure fast surface displacements in both the range and azimuth directions by using the cross-correlation optimization procedure, similar to optical feature tracking method, even if the interferometric phase is decorrelated [4]–[6]. It is not necessary to phase unwrapping procedure which is dominant error source of interferogram caused by high fringe rates in the case of large deformation areas; therefore, it can provide unambiguous ground displacements maps [7]. Especially, in the SAR offset tracking procedure, the signal-to-noise ratio (SNR) value of the correlation field is calculated to increase its confidence. The SAR offset tracking method's observation accuracy for ERS InSAR data with high correlation that is studied through comparison of the method with GPS observations is known to be limited to approximately 12 to 15 cm in azimuth direction [8]–[10]. Moreover, the SAR offset tracking measurement for ALOS PALSAR InSAR pair has the improved accuracy of about 7.1 cm [11].

However, the measurement performance of the method largely depends on the search kernel sizes, which denote the sizes of search window to estimate the range and azimuth offsets between reference and target SAR images. There is a trade-off between the resolution and accuracy of the SAR offset tracking measurement according to the search kernel sizes. When coherence is not retained due to large deformation, excessively small window sizes are unable to find its counterpart features in the other images. Thus, if the kernel size is small, the resolution of the displacement image is high, but the number of effective pixels is small because the SNR values is low for the entire image and the image quality in the parts of the large displacements is especially poor. On the other hand, if the kernel sizes are large, the number of effective pixels is large, but the resolution is low, so that the displacement map is distorted and the image quality is poor. Therefore, it is important to determine the proper kernel sizes in order to effectively observe the two-dimensional (2D) displacements using the SAR offset tracking method because there are many unreliable parts using only a single search kernel. However, up to now, the SAR offset tracking method has been applied by determining the proper kernel sizes in an experimental and empirical way.

To overcome the limits above, in this paper, an improved SAR offset tracking method based on multi-kernel processing is proposed. We focused on determining proper range of kernel sizes and generating optimal offset measurements through statistical processing based on the multiple pieces of offset measurements from the multiple search kernels to improve the trade-off between cross-correlation accuracy and resolution. Application and performance validation of the proposed approach were carried out by using ERS raw data spanning the 1999 Hector Mine earthquake and ALOS-2 PALSAR-2 raw data spanning the 2016 Kumamoto earthquake through a comparison with GPS data.

II. DATASET AND METHODS

To develop the improved SAR offset tracking method and obtain the optimized 2D displacement measurements, we firstly used the ERS-2 raw data pair (descending track 127 and frame 2907) acquired on September 15 and October 20, 1999. This descending co-seismic pair has the minimum possible time span of 35 days and it also has an extraordinarily short baseline of only 21 m. The image covers the epicenter of the Hector Mine earthquake, California (Mw of 7.1), which occurred on October 16, 1999. Thus, because the master and slave ERS-2 data are acquired on one month before and 4 days after the earthquake, respectively, the SAR offset tracking results represent cumulative displacements. This co-seismic ERS data pair was chosen because it was deemed most appropriate for this study for the following reasons: 1) GPS data is available to evaluate the performance of the proposed method [12]; 2) Previous SAR offset tracking displacements are available [8]–[10]; 3) large displacements exists [13]; 4) Interferometric coherence is high [14]. In addition, the proposed SAR offset tracking processing strategy was applied using the ALOS-2 PALSAR-2 SLC data (level 1.1) pair from descending orbits on March 7 and April 18, 2016. The additional test images include episodic strike-slip and normal faulting movement caused by the 2016 Kumamoto earthquakes (Mw $>$ 6) on April 14 and 15, 2016. Surface deformation accumulated by such events during that time resulted in large and complex deformation pattern in the SAR offset tracking results [15]. The results were verified by GPS in-situ measurements from the Geospatial Information Authority of Japan (GSI). Detailed location of GPS stations in the Hector Mine and Kumamoto can be found in [14] and [15], respectively. The system parameters [15], [16] and characteristics of the SAR offset tracking pairs in this study are summarized in Table 1.

The processing flow of this study is summarized in Fig. 1 and is composed of two main steps as follows:

1) SAR offset tracking processing: a) determination of initial constant offsets between master and slave single-look complex (SLC) images after common band filtering, b) offset tracking between the SLC pair using intensity cross-correlation from multiple search window sizes, and c) generation of range and azimuth displacement maps from the offset measurements according to the kernel sizes after applying multi-looking operation.
2) Multi-Kernel processing: a) decision of range to apply multi-kernel processing, and b) generation of the final range and azimuth displacements maps through computation of the average displacement map from multiple displacement maps according to the kernel sizes after removing outliers.

To generate precise displacement maps using the proposed method, SLC images were firstly generated from the ERS-2 and the ALOS-2 PALSAR-2 raw data. Then, initial constant range and azimuth offsets [see i_1 and i_2 in Fig. 2(a)] caused by orbital differences between the master and slave SLC images

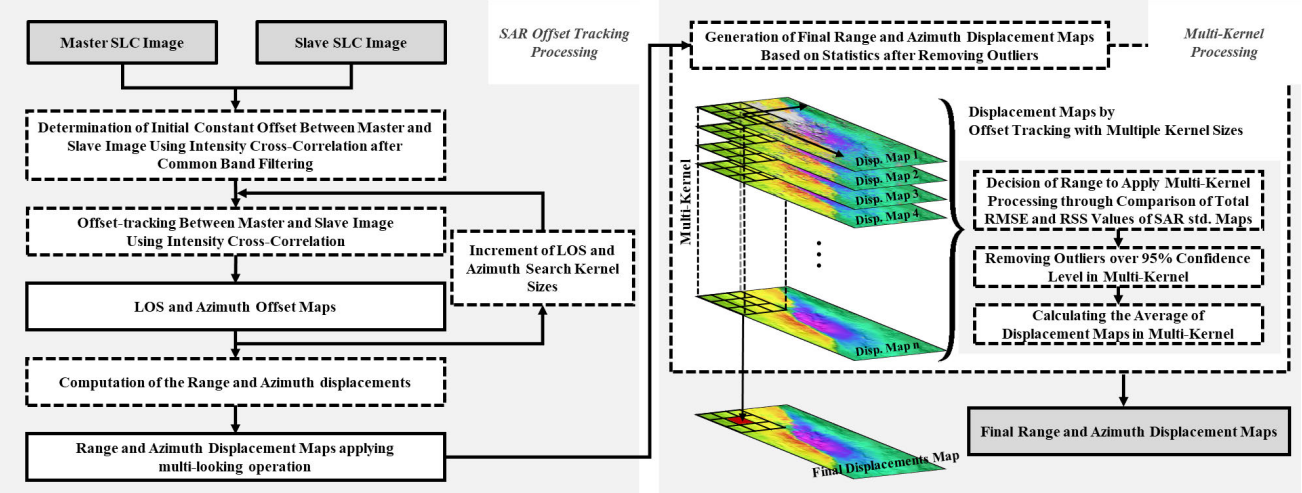

FIGURE 1. Detailed processing workflow that is proposed in this study. The proposed method is composed of two main steps: SAR offset tracking processing and Multi-kernel processing.

TABLE 1. System parameters and characteristics of SAR Offset tracking pairs used in this study.

Parameters	ERS-2	ALOS-2 PALSAR-2
Acquisition Date (yyyymmdd)	19990915[a] 19991020	20160307[a] 20160418
Effective Doppler Bandwidth (Hz)	1420	1515
Pulse Repetition Frequency (Hz)	1680	2000
Chirp Bandwidth (MHz)	15.6	84.0
Carrier Frequency (GHz)	5.300	1.258
Mean Incidence Angle (deg)	23	36
Effective Azimuth Antenna Dimension (m)	10	9.9
Azimuth Pixel Spacing (m)	4.0	2.1
Ground Range Pixel Spacing (m)	20.2	2.4
Azimuth Resolution (m)	5	3.8
Ground Range Resolution (m)	25	2.4
f_{DC}[b] (Hz)	49.6	-37.6
$B\perp$[c] (m)	-21	-121
B_t[d] (Days)	35	42

[a] Master image; [b] Doppler Centroid after azimuth common band filtering; [c] the perpendicular baseline; [d] the temporal baseline, which is the difference of SAR acquisition time.

were estimated by determining polynomial coefficients for offsets in both range and azimuth direction over the whole image based on intensity cross-correlation. It was implemented with large search kernel sizes assuming no displacement for large parts of the image. When applying the SAR offset tracking method, the initial constant offsets i_1 and i_2 are used to find the point of the slave image corresponding to the master image and to calculate the displacements in the search kernel for the common part. It is noted that estimation of the initial offset should be carried out accurately because it is one of the main error sources to calculate displacements from the pixel offset estimation. For more precise determination, we applied common band filtering in range and azimuth to raw data in order to improve the range spectra when the viewing angle of SAR is different and minimize the effects of the Doppler centroid difference on the azimuth spectra before this initial step [17], [18].

After initial offset estimation, the SAR offset tracking method used in [19] was applied to the SLC image pair. As shown in Fig. 2, the two-dimensional offsets over a grid of search kernels for a pair of SLC images S_1 and S_2 are estimated based on normalized intensity cross-correlation algorithm that seeks the correlation peak between search kernels from two SLC images. Data covering the search kernel with m × n (range × azimuth) pixels is extracted from each SLC image. Then, phase gradients are estimated and removed. Prior to calculate the cross-correlation value, the SLC data in search kernels are over-sampled by a factor of 2, or more using fast Fourier transforms (FFT) interpolation to improve somewhat the estimation of the peak location. As shown in Fig. 2(b), the normalized cross-correlation function $C(j_1, j_2)$ is defined by [19]:

$$C(j_1, j_2) = FFT^{-1}[I_1(j_1, j_2)\, I_2^*(i_1 + j_1, i_2 + j_2)] \quad (1)$$

where I_1 and I_2 are the normalized over-sampled SAR intensity data calculated from $\|S_1 S_1^*\|$ and $\|S_2 S_2^*\|$, respectively. The location of the correlation peak P' is estimated using a 2D quadratic least squares fit. When the correlation peak is found, the range and azimuth offsets can be determined by the offset vector between the search kernel's center P and the P'. The quality of the offset estimation is evaluated by computing the effective signal-to-noise ratio (SNR) by dividing the peak value of the cross-correlation coefficient by the standard deviation of the cross-correlation coefficients. When the SNR went below an assigned threshold, the data is removed as missing data.

In order to successfully calculate the offset from the SAR offset tracking, there should be a nearly identical features in the SAR image pair at the scale of the employed search

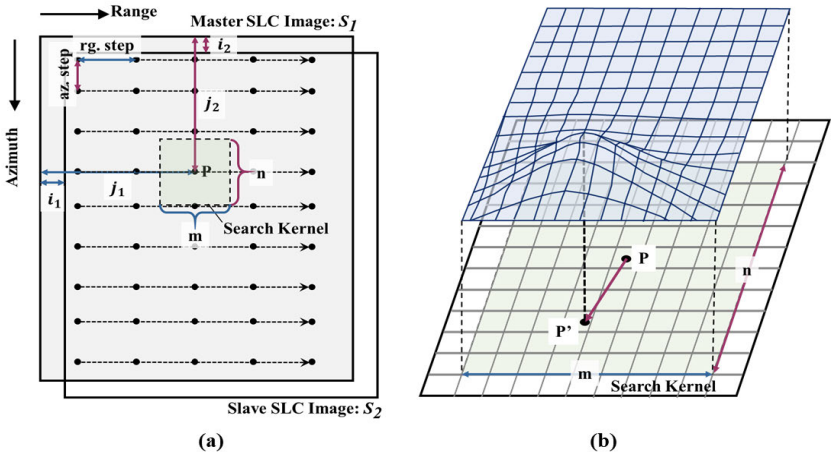

FIGURE 2. Schematic diagram of the (a) SAR offset tracking method and (b) correlation field. In (a), S_1 and S_2 indicate the master and slave SLC images, respectively. The initial constant range and azimuth offsets are i_1 and i_2. The green square areas in S_1 and S_2 are m × n (pixel) search window kernel in the range and azimuth directions, respectively. The offsets from the search kernel's center P is identified using the normalized cross-correlation function, which is given by Eq. (1). In (b), a complete correlation field has been built up and is shown as a correlation surface. The distance (d) between the center of the search window P and the location of the correlation peak P' is the estimated offset for location P.

kernel. Some of deformation on medium to high coherence areas can be well estimated from small to medium search kernel sizes. While others of deformation on low coherence areas due to large surface displacements require sufficient large search kernel sizes but oversized window sizes reduce resolution of displacements fields. In the SAR offset tracking processing, the search kernel sizes should be optimized. Thus, in case of the ERS-2 pairs, at each pixel location with steps are 3 pixels in range and 15 pixels in azimuth to obtain a pixel size of about 60 m × 60 m in ground range and azimuth, we experimentally used multiple search kernel sizes varying from 30 × 60 to 180 × 360 single-look pixels increasing the search kernel sizes of 10 pixels and 20 pixels in range and azimuth directions, respectively. In this way an almost squared area is considered and 16 range and 16 azimuth offset measurements are obtained. For the ALOS-2 PALSAR-2 pairs, we set the search kernel sizes varying from 32 × 32 to 384 × 384 pixels increasing the search kernel sizes of 32 pixels both range and azimuth directions with the sampling interval of 12 × 15 pixels for range and azimuth (∼30 m × 30 m in ground range and azimuth). In this way, 12 range and 12 azimuth SAR offset measurements are acquired. Then, all of the offset measurements were converted to displacements maps in meters in ground range and azimuth direction after multi-look operation considered the step sizes. The SNR threshold to accept offset value was set to 7.0 for ERS-2 pair and 4.0 for ALOS-2 PALSAR-2 pair; because the temporal and geometrical decorrelations are expected to be relatively large in the case of ALOS-2 PALSAR-2 pair (see the perpendicular and temporal baseline in Table 1). This SAR offset tracking processing requires intensive computation power and time. The computational analysis according to estimation kernel sizes can be found in [20].

To find optimized SAR offset tracking displacements maps from the trade-off between the accuracy and resolution according to the search kernel sizes, we devised multi-kernel processing considered the statistical properties of the multiple measurements. A multi-kernel is a moving window to estimate a final displacement map from multiple measurements by calculating the average of the multiple measurements after removing outliers. The multi-kernel averages the pixels within the multi-kernel from the SAR offset tracking results generated in the previous SAR offset tracking step after removing the outliers outside of 95 % confidence intervals. Although in the process of performing SAR offset tracking outliers were directly removed when below the SNR threshold values, outliers were removed once more in the multi-kernel processing because the outliers were not completely removed during the displacement estimation. For example, if there are 10 azimuth displacement maps obtained with different search kernel sizes, one pixel in the final azimuth displacements map estimated from the 3 × 3 multi-kernel is determined by calculating the average for 90 pixels after removing outliers outside of 95 % confidence intervals. To achieve more ideal results using a multi-kernel, multi-kernel processing using weighted-average of offset tracking results was also considered. Because there is a trade-off between measurement accuracy and resolution, it is difficult to determine relative importance and calculate weighting factor between accuracy and resolution. Moreover, there is a problem that when the weighting factor is used as the RMSE values of the GPS observation, because there may not be GPS observation data. Therefore, rather than considering the weighted-average, we approached by removing outliers and averaging the offset tracking results using multi-kernel that is a simple but proper way.

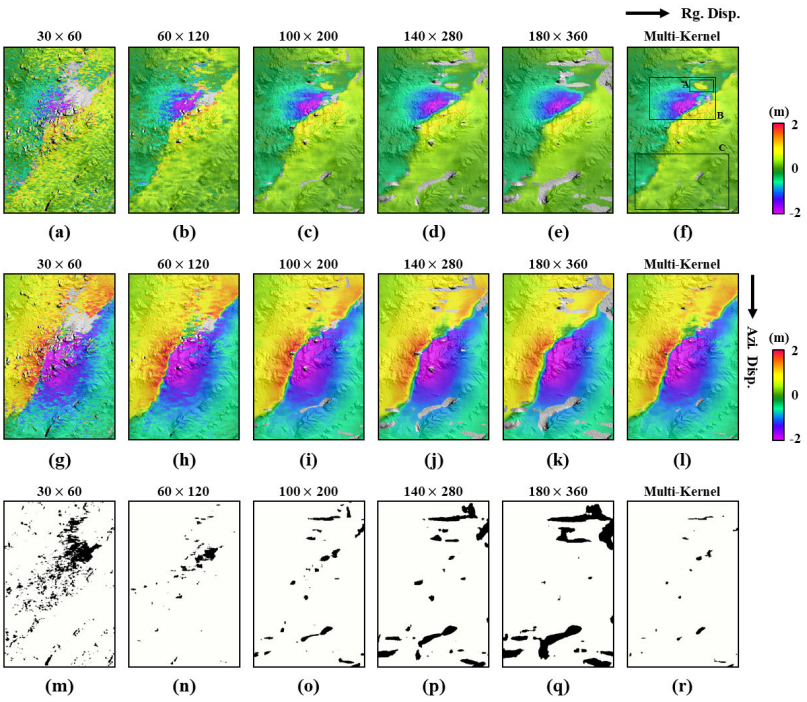

FIGURE 3. (a-e) Ground range displacement maps of the Hector Mine earthquake generated by using the SAR offset tracking method with a single search window kernel. (g-k) Azimuth displacement maps of the Hector Mine earthquake generated by using the SAR offset tracking method with a single search window kernel. The sizes of each search window kernel are shown above the figures. (f) and (l) range and azimuth displacement maps from multi-kernel processing with the multiple results illustrated to black filled box in Fig. 4, respectively. (m-r) Masked area shown in black where SNR value is lower than threshold value during SAR offset tracking processing.

In order to determine the range to apply the multi-kernel considering both the resolution and accuracy, we compared between each total RSS (root sum square) values of standard deviations of the SAR offset tracking measurements from 5 × 5 moving window and total RMSE (root-mean-square errors) errors between the SAR offset tracking measurements and GPS measurements. The start of the range to apply multi-kernel processing is based on the reduction in total RMSE value according to the kernel size that indicates measurement accuracy. The end of the range is defined as the kernel size before the total RSS value indicating the resolution converges to a specific value. It is very important to set the proper range to apply the multi-kernel. In case the GPS observations are not available, we also considered the proposed multi-kernel with all the offset tracking results. However, the optimal results could not be obtained because the noise of the result from the smaller kernel sizes and the degradation of the resolution of the result from the larger kernel sizes were considered. Thus, in the absence of GPS measurements, it is necessary to determine the range to apply the multi-kernel processing using only the resolution information according to the kernel sizes.

In the case of ERS-2 results, The RMSE values were calculated using 57 GPS data with correction errors for interseismic displacements of 0.25 cm or less in North and East directions among all 71 available GPS data in the study area [13]. Based on the comparison between total RMSE and total RSS values, 5 range and 5 azimuth SAR offset tracking results, which were estimated by the search window sizes from 80 × 160 to 120 × 240 pixels, were used to apply the multi-kernel. In the case of ALOS-2 PALSAR-2 results, we had to generate interseismic displacements using 12 points of GPS data in the study area to estimate RMSE values. For this purpose, the GPS data was divided into the before and after the earthquake, and the difference between each average was used as the final GPS in-situ measurements. Of the total 12 GPS observations, only 8 observations were available except for the masked areas in the SAR offset tracking results because of its low coherence. Through the comparison of RMSE and RSS values according to kernel sizes, we applied multi-kernel processing to 5 range displacement maps and 5 azimuth displacements maps that were estimated by the search window sizes from 192 × 192 pixels to 320 × 320 pixels.

III. RESULTS AND DISCUSSION

A. APPLICATION TO THE 1999 HECTOR MINE EARTHQUAKE

The 16 range and 16 azimuth displacement maps were obtained from the SAR offset tracking method using multiple

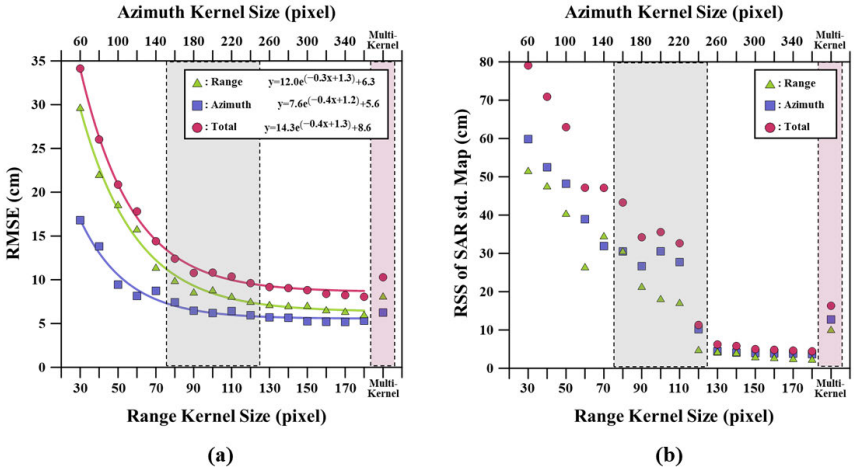

FIGURE 4. Determination of the range to apply the multi-kernel considering both the accuracy and the resolution according to the search kernel sizes. (a) Comparison of total RMSE (root-mean-square errors) errors between the SAR offset tracking measurements and 56 GPS measurements. (b) Comparison between each total RSS (root sum square) vales of standard deviations of the SAR offset tracking measurements. In (a) and (b), the green triangles, blue squares, and red circles indicate the SAR offset tracking measurements in range, azimuth, and total direction, respectively. From (a) and (b), the proper range to apply the multi-kernel were determined from 80 × 160 to 120 × 240 pixels, where the black filled box. Moreover, the red filled box presents the multi-kernel results in both (a) and (b).

search kernel sizes varying from 30 × 60 to 180 × 360 pixels increasing the search kernel sizes of 10 pixels and 20 pixels in range and azimuth directions, respectively. Fig. 3 presents some of the ground range displacement maps [see Fig. 3(a)–(e)] and azimuth displacement maps [see Fig. 3(g)–(k)] estimated from the SAR offset tracking method. The displacement maps were presented using a fringe pattern in a rainbow color, and one fringe of each displacement map corresponds to surface deformation of 4 m.

From the offset tracking results, the smaller kernel sizes [see Fig. 3(a), (b) and (g), (h)], the better resolution of displacement observations in local areas. Therefore, it is confirmed that the strike slip fault line of the Hector Mine earthquake is clearer than others. However, the smaller the kernel sizes, the lower the SNR value that indicates the quality of the offset estimation in the region where the large surface displacement. As a result, the number of effective pixels is small, so that the measurement density is low, and outliers appear in the observation results [see Fig. 3(m) and (n)]. Therefore, if the kernel sizes are small, it can be predicted that the observation accuracy is low.

On the other hand, as the sizes of the kernel increase [see Fig. 3(d), (e) and (j), (k)], offset tracking is performed on more pixels in each pixel location of offset estimation. As a result, it is possible to confirm that the resolution of the displacement observations is low and the fault line is distorted and becomes unclear. Moreover, as the size of the search kernel increases, the number of pixels to be masked gradually increases where the SNR is lower than the threshold 7.0 [see Fig. 3(p) and (q)]. However, the measurement density is high at the part where the surface displacement is large. In this case, the resolution of the image is low, but it is predicted that the observation accuracy will be high because the noise is less.

Thus, the surface displacement image generated using only a single kernel with small or large kernel sizes cannot be regarded as a reliable result satisfying both the measurement density and the accuracy due to the trade-off relationship. Therefore, we proposed multi-kernel processing which can obtain optimal observation result. The proposed method is a statistical technique to treat the unreliable parts of the measurement density and accuracy due to the trade-off relationship according to the kernel sizes.

Fig. 4 is a quantitative analysis of the observation accuracy and resolution according to the search kernel sizes of the SAR offset tracking method. It was done for the purpose of determining the coverage of the proposed multi-kernel processing. Fig. 4(a) shows the RMSE values between SAR offset tracking results and 57 GPS in-situ measurements, and Fig. 4(b) shows the RSS values of the standard deviation map of SAR offset tracking measurements. In Fig. 4(a), it can be seen that the RMSE values decrease in the form of an exponential function as the kernel sizes increase. When comparing the total RMSE values according to kernel sizes, the reduced amount of the total RMSE values before the kernel sizes of 80 × 160 pixels was about 2∼3 cm, and it is reduced to within about 1.5 cm from 80 × 160 pixels. The total RMSE value of 80 × 160 pixels is 12.4 cm, and as the kernel size increases, the total RMSE values decrease to approximately 8 cm. As shown in Fig 4(b), the total RSS values were less than 5 cm after the kernel sizes of 120 × 240 pixels. This is because as the size of the kernel increases,

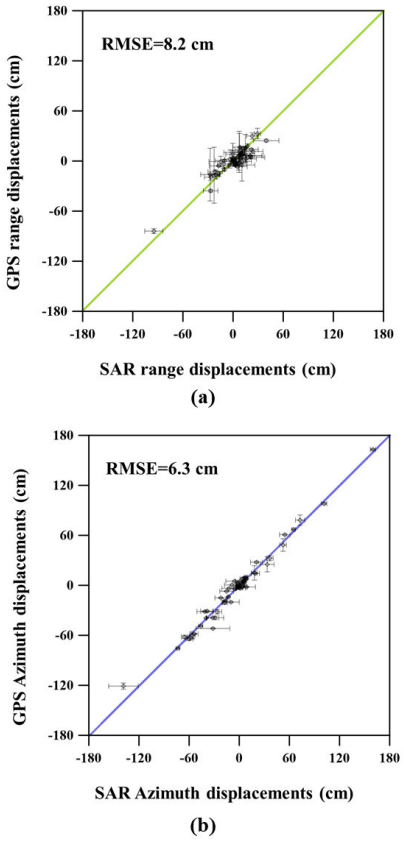

FIGURE 5. Comparison of 2D displacements estimated from the proposed SAR offset tracking method with GPS displacements at 56 stations on the Hector Mine. (a) Range component. (b) Azimuth component. Squares and bars denote uncertainties of proposed SAR offset tracking and GPS measurements at two standard deviations, respectively.

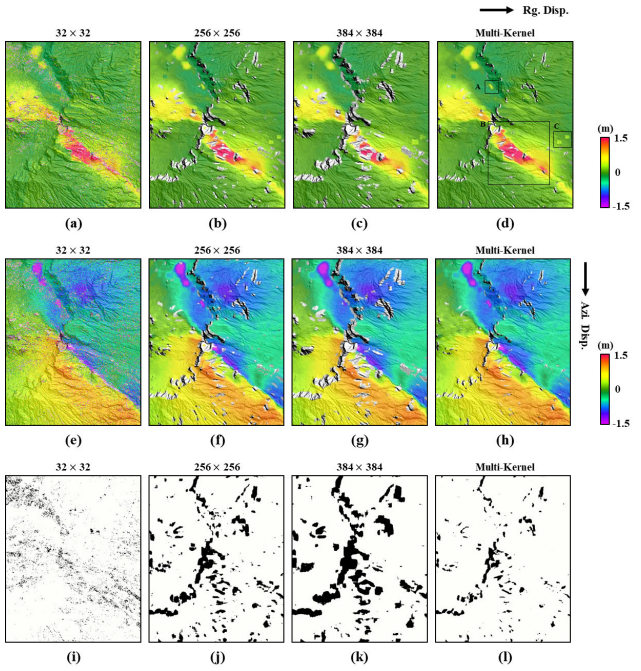

FIGURE 6. (a-c) Ground range displacement maps of the 2016 Kumamoto earthquake generated by using the SAR offset tracking method with a single search window kernel. (e-g) Azimuth displacement maps of the 2016 Kumamoto earthquake generated by using the SAR offset tracking method with a single search window kernel. The sizes of each search window kernel is shown above. (d) and (h) range and azimuth displacement maps from multi-kernel processing with the multiple results illustrated to black filled box in Fig. 7, respectively. (i-l) Masked area shown in black where SNR value is lower than threshold value during SAR offset tracking processing.

the offsets between reference and target SAR images are estimated based on more pixels, resulting in spatial smoothing in the offset tracking result. The RSS value converges to a small value of approximately 5 cm from 130 × 260 pixels. It means that the degradation of the resolution becomes severe, so that the detailed displacement cannot be observed [see Fig. 3(d), (j) and (e), (k)]. However, the amount of noise in the image is small from 130 × 260 pixels, so that the RMSE value is low and the observation accuracy is high [see Fig. 4(a)]. Thus, considering this trade-off between observation accuracy and resolution, multi-kernel processing was applied to with search window kernel sizes ranging from 80 × 160 pixels to 120 × 240 pixels.

Fig. 3(f) and (l) represent the final range and azimuth displacement maps generated by multi-kernel processing, respectively. This is the result of moving 3 × 3 multi-kernel to eliminate outliers that exceed 95 % confidence intervals and calculate the average of 5 displacement maps along range and azimuth directions respectively obtained by the search kernel from 80 × 160 pixels to 120 × 240 pixels. Comparing the box A part shown in Fig. 3(f) when the kernel sizes are small [see Fig. 3(a) and (b)] and large [see Fig. 3(d) and (e)], it can be seen that the SNR values are all low and the parts are masked out as unreliable observations [see Fig. 3(m), (n), (p), and (q)]. In the case of the box B part in Fig. 3(f), the range displacement pattern expressed in purple color is composed of two patterns. However, when the kernel sizes are small, the surface displacement is not clearly observed because of low SNR, and when the kernel sizes are large, it is confirmed that the displacement pattern is measured in almost one lump due to the resolution degradation. Moreover, in case of box C in Fig. 3(f), when the kernel sizes are small, the masked areas are small due to the high measurement density, but when the kernel sizes are large, the masked areas are increased. Comparing the multi-kernel result [see Fig. 3(f)] and the result of using a single search kernel of 100 × 200 pixels [see Fig. 3(c)] that can be said to be middle in a trade-off relationship between resolution and accuracy, in the case of box A and B, the surface displacements were similar, but the multi-kernel result is less masked and less noise [see Fig. 3(o) and (r)]. This is due to the fact that the final surface displacement maps are statistically processed using multi-kernel. It is also possible to check the RSS values of the multi-kernel result of Fig. 4(b). Moreover, in the box C part, it can be seen that the masked areas are significantly reduced in the multi-kernel result. This is because the statistical processing is performed through the proposed multi-kernel processing using the results with a single kernel containing unreliable

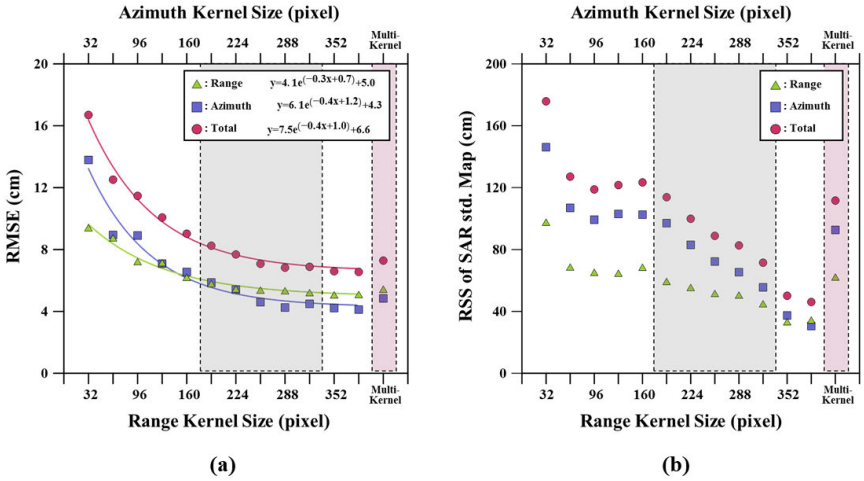

FIGURE 7. Determination of the range to apply the multi-kernel considering both the accuracy and the resolution according to the search kernel sizes. (a) Comparison of total RMSE (root-mean-square errors) errors between the SAR offset tracking measurements and 8 GPS measurements. (b) Comparison between each total RSS (root sum square) vales of standard deviations of the SAR offset tracking measurements. In (a) and (b), the green triangles, blue squares, and red circles indicate the SAR offset tracking measurements in range, azimuth, and total direction, respectively. From (a) and (b), the proper range to apply the multi-kernel were determined from 192 × 192 to 320 × 320 pixels, where the black filled box. Moreover, the red filled box presents the multi-kernel results in both (a) and (b).

parts. In other words, it is possible to mitigate the unreliable parts and derive the most reliable and optimal results.

Fig. 5 compares the final displacements along the range and azimuth directions generated by the proposed multi-kernel processing with the 57 GPS in-situ measurements. The RMSE between the proposed SAR offset tracking and GPS in the range and azimuth components are 8.2 and 6.3 cm, respectively that includes up to 3 cm of post-seismic displacements because the GPS data includes post-seismic displacements spanning 6 and 3 months after the earthquake [12]. In particular, the accuracy of azimuth direction displacements is considerably better than the accuracy of ∼12-15 cm observed in previous SAR offset tracking study [8]–[10]. Moreover, the accuracy of the azimuth direction is similar to that of the azimuth direction accuracy observed by the MAI technique, which is about 5.5 cm, corresponding to only 1.1% of the azimuth resolution of the ERS SAR system [10], [21].

This is because the proposed SAR offset tracking method improves the coherence of the SAR offset tracking displacements by the following: 1) common band filtering is performed before SAR offset tracking to improve the offset tracking accuracy; 2) SAR offset tracking is implemented considered very dense areas to finely find displacements; and 3) multi-kernel processing is applied when calculating displacements to improve the measurement density. When comparing the RMSE values according to kernel sizes in Fig. 4(a), the measurement accuracy of the multi-kernel result [see red filled box in Fig. 4(a)] is lower than the results with kernel sizes greater than 130 × 260 pixels. However, when the kernel sizes are more than 130 × 260 pixels, the result of RMSE values are excessively small due to excessive resolution degradation. In addition, although we have found the appropriate search window sizes and created displacement maps using only the single kernel in an experimental and empirical way [like Fig. 3(c) and (i)], there are masking and noise parts due to low SNR values in the results [see Fig. 3(o)]. In conclusion, it is possible to derive observation results with high measurement density and accuracy through the proposed SAR offset tracking processing strategy. It is demonstrated that the most optimal result can be obtained by the proposed method improving the trade-off relationship between resolution and measurement accuracy.

B. APPLICATION TO THE 2016 KUMAMOTO EARTHQUAKE

Fig. 6 shows some of the range displacement maps [see Fig. 6(a)-(c)] and azimuth displacement maps [see Fig. 6(e)-(g)] among the multiple SAR offset tracking results. Fig. 6(a)-(c) and Fig. 6(e)-(g) are generated by the size of search window kernel in the range and azimuth directions of 32 × 32, 256 × 256, and 384 × 384 pixels. The displacement maps were presented using a fringe pattern in a rainbow color, and one fringe of each displacement map corresponds to surface deformation of 3 m.

In these SAR offset tracking results for the Kumamoto earthquake, it is also confirmed that there is the trade-off relationship between the resolution and observation accuracy according to the SAR offset tracking kernel sizes. When the kernel sizes are small [see Fig. 6(a) and (e)], it is possible to effectively observe local displacements at a high resolution. However, since there are many outliers in the observation results, it can be predicted that the observation accuracy of

the image is low [see Fig. 6(i)]. On the other hand, as the kernel size increases [see Fig. 6(c) and (g)], the resolution of the image is lower than that of the case when the kernel sizes are smaller, and the land surface displacements such as landslide are distorted. Moreover, when the kernel sizes are large, the masked pixels increase due to the low SNR values of intensity cross-correlation, resulting in a large number of empty portions in the image [see Fig. 6(k)]. However, since the offset is estimated with a large kernel, it can be predicted that the observation accuracy is high due to the reduction of the outliers in the observation result. Thus, it is also necessary to improve the trade-off relationship to obtain a reliable result satisfying both the measurement density and accuracy.

Fig. 7 is a quantitative analysis of the observation accuracy and resolution according to the search kernel sizes of the SAR offset tracking method. Fig. 7(a) shows the RMSE values between SAR offset tracking displacements and 8 GPS in-situ measurements, and Fig. 7(b) shows the RSS values of the standard deviation map of SAR offset tracking measurements according to the kernel sizes. In Fig. 7(a), the RMSE values are reduced as an exponential function according to the kernel sizes. When the total RMSE values according to the kernel sizes are compared, the amount of decrease in the total RMSE value before displacement estimated kernel sizes of 192 × 192 pixels were about 1 to 4 cm, and it is reduced to within about 0.04 to 0.7 cm from 192 × 192 pixels kernel sizes. The total RMSE value of 192 × 192 pixels is about 8.3 cm, and as the kernel sizes increase, the total RMSE value decreases to approximately 6.6 cm. As shown in Fig. 4(b), the total RSS value was less than 50 cm after the kernel sizes of 352 × 352 pixels. This value is greater than the total RSS values of Hector Mine earthquake which are approximately 5 cm when the search kernel sizes are large [see Fig. 4(b)]. Compared with the Hector Mine earthquake, the total RSS values are as large as 50 cm despite the large search kernel sizes because the Kumamoto earthquake included a large amount of local surface displacements such as landslides. Tough the RMSE values converge from 320 × 320 pixels [see Fig, 7(a)], it can be confirmed that the RSS values indicating the image resolution is continuously decreased.

Considering the trade-off of between observation accuracy and resolution, as shown in Fig. 7, the multi-kernel processing was applied to displacement maps generated from a search window kernel sizes of 192 × 192 pixels to 320 × 320 pixels. Fig 6(d) and (h) shows the final displacement map of the Kumamoto earthquake generated by the proposed multi-kernel SAR offset tracking method. A qualitative assessment was carried out comparing the area of boxes A, B, and C in the final range displacement map [see Fig. 6(d)] with other results according to the kernel sizes [see Fig. 6(a)-(c)]. When the kernel sizes are small [see Fig. 6(a)], it contains values greater than 1.5 m in the local area of box A part that can be seen as noise. In case of medium kernel sizes and final displacement result [see Fig. 6(b) and 6(d)], the value of 1.5 m or more is reduced because the displacement is estimated with more surrounding pixels. Especially in case

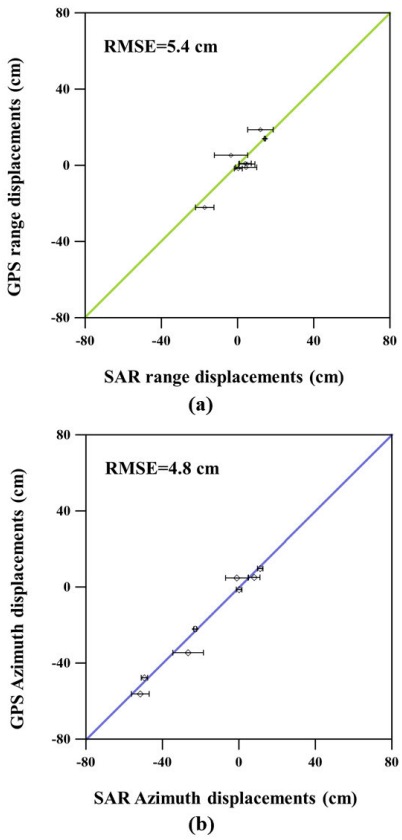

FIGURE 8. Comparison of 2D displacements estimated from the proposed SAR offset tracking method with GPS displacements at available 8 stations in the Kumamoto area. (a) Range component. (b) Azimuth component. Squares and bars denote uncertainties of proposed SAR offset tracking at two standard deviations.

of the kernel sizes are large [see Fig. 6(c)], it can be seen that the local surface displacement of box A is missing. For the fault area in box B part, the final surface displacement image is less masked and less noisy than other results generated using a single kernel [see Fig. 6(l)]. Thorough the multi-kernel processing, it is possible to obtain high quality results. This means that the proposed multi-kernel processing can provide the most reliable results in areas with large surface displacement. However, as in the case of Box C part, artificial kernel-shaped displacement can be measured as kernel sizes increase. In the SAR offset tracking process, if there is a part that is not outliers but has a much larger displacement than the surrounding pixels, the displacement is incorrectly estimated. Since the normalized cross-correlation function is obtained while moving the kernel, if such displacement exists, the displacement is incorrectly estimated to be an artificial kernel-shaped form. It is present ranged from 96 × 96 kernel sizes. As the kernel sizes increase, the size of this artificial displacement increases. On the other hand, the artificial kernel-shaped displacement did not appear in the azimuth direction because the displacement was less noisy than the range direction.

It seems to be a problem in estimating the displacement using SAR offset tracking caused by the presence of outliers in one of the SLC pairs.

Fig. 8 represents a comparison of the final displacements along the range and azimuth direction generated by the proposed multi-kernel processing with a total of 8 GPS observations available in the study area. The RMSE between the proposed SAR offset tracking and GPS in the range and azimuth components are 5.4 and 4.8 cm, respectively. The results are corresponding to 2.25 % and 2 % of the ground range and azimuth resolution of the ALOS-2 PALSAR-2 system [see Table 1]. In conclusion, through the proposed method, a precise observation is effectively possible in large and complex surface displacement areas.

IV. CONCLUSION

An improved SAR offset tracking method is proposed to find an optimized measurement from the trade-off between the observation accuracy and resolution according to search window kernel sizes. The proposed method based multi-kernel processing is that 1) calculates multiple offset measurements and 2) determines a precise measurement from the statistical properties of the multiple measurements. Its performance has been validated by using the ERS-2 co-seismic measurement and GPS measurement in the event of the Hector Mine Earthquake. In addition, the proposed method has been applied and verified using ALOS-2 PALSAR-2 pair in the event of the 2016 Kumamoto earthquake. Through the multi-kernel SAR offset tracking processing, it is possible to statistically integrate more observable displacement components according to each kernel sizes. In addition, this process has the effect of reducing unreliable parts by statically overlapping.

Moreover, through comparison between the SAR and GPS displacements, in case of the ERS-2 pair, the achieved measurement accuracies in the range and azimuth directions were about 8.2 cm and 6.3 cm, respectively. In case of the ALOS-2 PALSAR-2 pair, it was acquired 5.4 cm and 4.8 cm respectively. It means that the proposed method can measure the large surface displacements with the observation accuracy of about 8 to 6 cm for the ERS-2 pair and about 5 cm for the ALOS-2 PALSAR-2 in both the range and azimuth directions. Thus, the proposed method can produce the reliable result from the trade-off relationship between observation accuracy and resolution according to the kernel sizes, allowing for better observation of surface displacement than the tradition single kernel SAR offset tracking.

If the SAR image resolution and the size of the displacements pattern are similar to our application cases, the search window sizes applying the multi-kernel processing used in this study can be applied to other cases. Otherwise, it is necessary to analyze SAR offset tracking results according to kernel sizes and determine the range to apply multi-kernel as in this study. Research to develop more robust methodologies will be undertaken in the future study.

REFERENCES

[1] A. K. Gabriel, R. M. Goldstein, and H. A. Zebker, "Mapping small elevation changes over large areas: Differential radar interferometry," *J. Geophys. Res.*, vol. 94, pp. 9183–9191, Jul. 1989.
[2] D. Massonnet and K. L. Feigl, "Radar interferometry and its application to changes in the Earth's surface," *Rev. Geophys.*, vol. 36, no. 4, pp. 441–500, Nov. 1998.
[3] Z. Lu, O. Kwoun, and R. Rykhus, "Interferometric synthetic aperture radar (InSAR): Its past, present and future," *Photogramm. Eng. Remote Sens.*, vol. 73, no. 3, pp. 217–221, Mar. 2007.
[4] H. Rott, M. Stuefer, A. Siegel, P. Skvarca, and A. Eckstaller, "Mass fluxes and dynamics of Moreno Glacier, Southern Patagonia Icefield," *Geophys. Res. Lett.*, vol. 25, no. 9, pp. 1407–1410, 1998.
[5] T. Strozzi, A. Luckman, T. Murray, U. Wegmüller, and C. L. Werner, "Glacier motion estimation using SAR offset-tracking procedures," *IEEE Trans. Geosci. Remote Sens.*, vol. 40, no. 11, pp. 2384–2391, Nov. 2002.
[6] S.-H. Chae, W.-J. Lee, H.-S. Jung, and L. Zhang, "Ionospheric correction of L-band SAR offset measurements for the precise observation of glacier velocity variations on Novaya Zemlya," *IEEE J. Sel. Topics Appl. Earth Observ. Remote Sens.*, vol. 10, no. 8, pp. 3591–3603, Aug. 2017. doi: 10.1109/JSTARS.2017.2690799.
[7] R. Michel and E. Rignot, "Flow of Glaciar Moreno, Argentina, from repeat-pass Shuttle Imaging Radar images: Comparison of the phase correlation method with radar interferometry," *J. Glaciol.*, vol. 45, no. 149, pp. 93–100, Jan. 1999.
[8] Y. Fialko, M. Simons, and D. Agnew, "The complete (3-D) surface displacement field in the epicentral area of the 1999 M_w7.1 hector mine Earthquake, California, from space geodetic observations," *Geophys. Res. Lett.*, vol. 28, no. 16, pp. 3063–3066, Aug. 2001.
[9] S. Jónsson, H. Zebker, P. Segall, and F. Amelung, "Fault slip distribution of the 1999 Mw 7.1 hector mine, California, Earthquake, estimated from satellite radar and GPS measurements," *Bull. Seismol. Soc. Amer.*, vol. 92, no. 4, pp. 1377–1389, 2002.
[10] H. S. Jung, Z. Lu, and L. Zhang, "Feasibility of along-track displacement measurement from sentinel-1 interferometric wide-swath mode," *IEEE Trans. Geosci. Remote Sens.*, vol. 51, no. 1, pp. 573–578, Jan. 2013.
[11] D. T. Sandwell, D. Myer, R. Mellors, M. Shimada, B. Brooks, and J. Foster, "Accuracy and resolution of ALOS interferometry: Vector deformation maps of the Father's day intrusion at Kilauea," *IEEE Trans. Geosci. Remote Sens.*, vol. 46, no. 11, pp. 3524–3534, Nov. 2008.
[12] D. C. Agnew, S. Owen, Z.-K. Shen, G. Anderson, J. Svarc, H. Johnson, K. E. Austin, and R. Reilinger, "Coseismic displacements from the hector mine, California, Earthquake: Results from survey-mode global positioning system measurements," *Bull. Seismol. Soc. Amer.*, vol. 92, no. 4, pp. 1355–1364, 2002.
[13] J. Behr *et al.*, "Preliminary report on the 16 October 1999 M 7.1 hector mine, California, Earthquake," *Seismol. Res. Lett.*, vol. 71, no. 1, pp. 11–23, 2000.
[14] D. T. Sandwell, L. Sichoix, D. Agnew, Y. Bock, and J.-B. Minster, "Near real-time radar interferometry of the Mw 7.1 hector mine Earthquake," *Geophys. Res. Lett.*, vol. 27, no. 29, pp. 3101–3104, 2000.
[15] W.-K. Baek, H.-S. Jung, and S.-H. Chae, "Feasibility of ALOS2 PALSAR2 offset-based phase unwrapping of SAR interferogram in large and complex surface deformations," *IEEE Access*, vol. 6, pp. 45951–45960, 2018.
[16] H.-S. Jung, W.-J. Lee, and L. Zhang, "Theoretical accuracy of along-track displacement measurements from multiple-aperture interferometry (MAI)," *Sensors*, vol. 14, no. 9, pp. 17703–17724, 2014.
[17] F. Gatelli, A. M. Guamieri, F. Parizzi, P. Pasquali, C. Prati, and F. Rocca, "The wavenumber shift in SAR interferometry," *IEEE Trans. Geosci. Remote Sens.*, vol. 32, no. 4, pp. 855–865, Jul. 1994.
[18] H.-S. Jung, J.-S. Won, and S.-W. Kim, "An improvement of the performance of multiple-aperture SAR interferometry (MAI)," *IEEE Trans. Geosci. Remote Sens.*, vol. 47, no. 8, pp. 2859–2869, Aug. 2009.
[19] C. Werner, U. Wegmüller, T. Strozzi, and A. Wiesmann, "Precision estimation of local offsets between pairs of SAR SLCs and detected SAR images," in *Proc. IGARSS*, 2005, pp. 4803–4805.
[20] S.-H. Hong, "Parallel computing on intensity offset tracking using synthetic aperture radar for retrieval of glacier velocity," *Korean J. Remote Sens.*, vol. 35, no. 1, pp. 29–37, 2019.
[21] N. B. D. Bechor and H. A. Zebker, "Measuring two-dimensional movements using a single InSAR pair," *Geophys. Res. Lett.*, vol. 33, no. 16, Aug. 2006, Art. no. L16311. doi: 10.1029/2006GL026883.

SUNG-HO CHAE received the M.S. degree in geoinformatics from the University of Seoul, South Korea, in 2016, where he is currently pursuing the Ph.D. degree with the Department of Geoinformatics. His research interests include improving measurement performance of the conventional SAR offset tracking method and advanced three-dimensional surface deformation mapping by the integration of interferometric SAR (InSAR), and multiple-aperture InSAR (MAI) measurements. He currently focuses on retrieving three-dimensional glacier motions using the InSAR, MAI, and SAR offset tracking methods.

WON-JIN LEE received the M.S. and Ph.D. degrees in geoinformatics from the University of Seoul, Seoul, South Korea, in 2010 and 2015, respectively. He is currently a Principal Researcher with the Environmental Satellite Center, National Institute of Environmental Research, South Korea. His research interests include estimation and correction of ionospheric effects on the InSAR processing and performance improvements of the surface deformation measurement from the InSAR and multi-temporal InSAR (MTInSAR) techniques. He is currently focusing on the development of InSAR methods to assess and predict risks associated with geophysical hazards.

WON-KYUNG BAEK was born in Daegu, South Korea, in 1991. He received the B.S. and M.S. degrees in geoinformatics and remote sensing from the University of Seoul, South Korea, in 2015 and 2017, respectively, where he is currently pursuing the Ph.D. degree in geoinformatics and remote sensing.

His research interests include multi-temporal and three-dimensional ground deformation measurements using phase- and pixel-based SAR measurement approaches, error mitigation in the SAR based ground deformation measurements, and efficient procedure to unwrap large and complex SAR interferograms using offset tracking.

HYUNG-SUP JUNG (M'09–SM'16) received the M.S. degree in geophysics and the Ph.D. degree in remote sensing from Yonsei University, Seoul, South Korea, in 1998 and 2007, respectively. He is currently an Associate Professor with the Department of Geoinfomatics, University of Seoul. His primary research interests include development of algorithms related to synthetic aperture radar (SAR), SAR interferometry (InSAR), multiple-aperture InSAR (MAI), and multi-temporal InSAR (MTInSAR), automated geometric correction of multi-sensor images, and multi-sensor image processing and fusion, thermal remote sensing, and multi-temporal optical and thermal sensing. He has been developing algorithms for remote sensing applications related to 3D deformation mapping by combining MAI and InSAR, and 2D surface velocity estimation by combining MAI and along-track interferometry (ATI), MAI-based ionospheric correction of radar interferograms, multi-sensor fusion by the integration of optic and SAR, SAR and thermal, and optic and thermal images, automated geometric correction for optic and SAR images, and Earth's surface variation monitoring, such as urban subsidence monitoring, glacier monitoring, volcano monitoring, deforestation monitoring, forest mapping, forest fire mapping, and snow depth estimation.